Absolute x-ray calibration of laser-produced plasmas using a CCD linear array and a focusing crystal spectrometer

Alexander P. Shevelko*[a], Larry V. Knight**[b], Quan Wang [b], and Oleg F. Yakushev [a]
[a]Optical Division, P. N. Lebedev Physical Institute; [b]Deparment of Physics and Astronomy, BYU

ABSTRACT

Absolute x-ray calibration of laser-produced plasmas was performed using a CCD linear array and a focusing crystal spectrometer. The plasmas were created by a *Nd* glass laser (0.53 μm/10 J/2 ns) and a high repetition rate *Nd-YAG* laser (0.53 μm/200 mJ/3 ns/10 Hz). A commercial CCD (Toshiba model TCD 1304AP) was used for x-ray detection. The CCD linear array has 3724 pixels (8 μm width and 200 μm height) giving a total length of ~30 mm. First the CCD detector was absolutely calibrated using laser-produced plasmas and an Fe^{55} isotope source. The sensitivity of the detector was about two orders of magnitude higher than x-ray photographic film (Kodak RAR 2492). The CCD detector was used for monitoring the absolute x-ray yield, for finding the optimal focal position, for estimating the flux density on the target and for measuring the electron temperature of the plasma. In combination with a focusing von Hamos spectrometer (curved mica and graphite crystals, radius of curvature R = 20 mm) the detector was used for absolute spectral measurements and determination of the plasma parameters. This spectrometer is promising for absolute spectral measurements of x-ray radiation of low-intensity sources and for numerous practical applications (e.g., x-ray fluorescence analysis and EXAFS).

Keywords: laser-produced plasmas, x-ray spectroscopy, CCD, x-ray crystal focusing spectrometers

1. INTRODUCTION

Recently, charge coupled devices (CCDs) have found widespread use in fundamental research and practical applications as active recording detectors in soft x-ray imaging systems.[1, 2] CCD x-ray detectors have the advantages of high sensitivity, good signal-to-noise ratio, wide dynamic range, and good spatial resolution. In the form of a two-dimensional multichannel detector, CCDs are a suitable replacement for photographic film in spectroscopic instruments. The x-ray sensitive CCD is a good real-time detector with known quantum efficiency and linear response with no need of complex developing processes. Examples can be found in [3-5] where CCDs were used in flat and spherical crystal spectrometers for x-ray spectroscopy of laser-produced plasmas.

The maximum efficiency of x-ray spectroscopic devices can be achieved when a CCD is used in the focusing schemes of crystal x-ray spectrometers. One of these is the von Hamos scheme.[6, 7] This scheme has several advantages—the most important being high efficiency in a wide spectral range. In the von Hamos geometry x-ray spectra are formed on the spectrometer axis. Thus, it is a possible to use a CCD linear array as an x-ray detector.

In this research, a low cost, commercial CCD linear array was used for absolute x-ray calibration and for monitoring the x-ray parameters of laser-produced plasmas. In combination with a focusing crystal von Hamos spectrometer, this detector was used for absolute spectral measurements and the determination of the plasma parameters. This compact device is promising for absolute spectral measurement of x-ray radiation from low intensity sources and for numerous practical applications (x-ray fluorescence analysis, EXAFS, etc.).

2. VON HAMOS SPECTROMETER

In the von Hamos scheme,[6, 7] a crystal is bent into a cylindrical surface. The x-ray source and the detector plane lie on the cylinder axis (see Fig. 1). The crystal diffracts x-rays with different wavelengths according to the Bragg law. Each wavelength, after diffraction from the crystal arc, is focused to a point lying on the spectrometer axis. This focusing geometry gives high spectrometer efficiency.

*Alexander Shevelko. Optical Division, P.N.Lebedev Physical Institute of the Russian Academy of Sciences, Leninsky Pr.53, Moscow 117924, Russia. Tel. +7 095 1326951, fax +7 095 135 2408, e-mail: ashev@mail1.lebedev.ru
**Larry Knight. Department of Physics and Astronomy, BYU, Provo, UT 84602. Tel. (801) 378 2186, fax: (801) 378 2265, e-mail: knight@physics.byu.edu

Applications of X Rays Generated from Lasers and Other Bright Sources II,
George A. Kyrala, Jean-Claude J. Gauthier, Editors, Proceedings of SPIE Vol. 4504 (2001)
© 2001 SPIE · 0277-786X/01/$15.00

Downloaded From: http://proceedings.spiedigitallibrary.org/ on 03/27/2014 Terms of Use: http://spiedl.org/terms

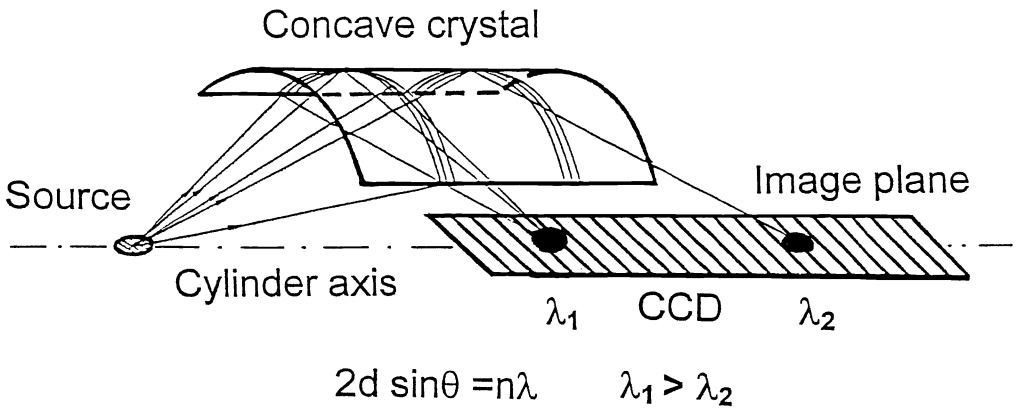


Fig. 1. Schematic diagram of the von Hamos spectrometer.

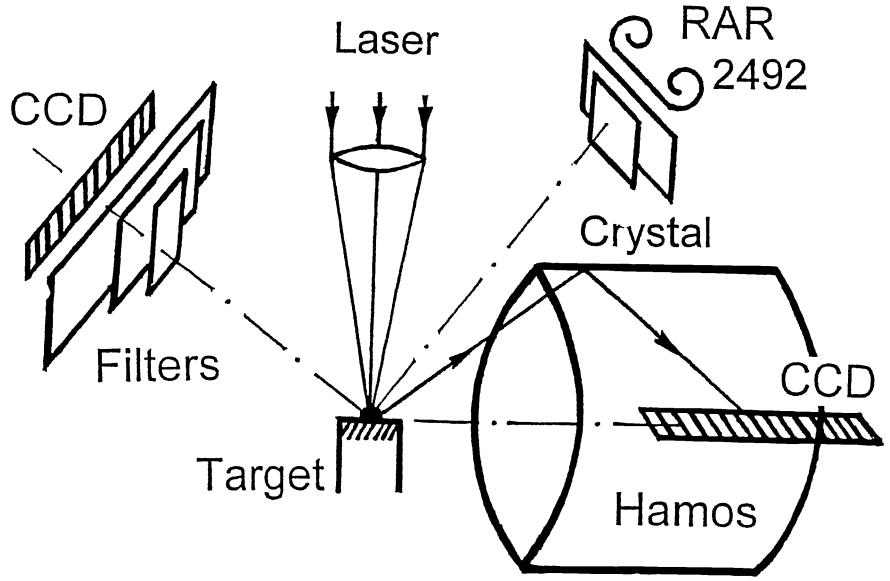


Fig. 2. Schematic diagram of the experimental geometry.

Downloaded From: http://proceedings.spiedigitallibrary.org/ on 03/27/2014 Terms of Use: http://spiedl.org/terms

The width of the spectral band in the von Hamos geometry depends on the length of the crystal in the dispersion direction. For a long crystal, the wavelength band $\Delta\lambda$ can be wide. Each wavelength in this band is focused to a unique spot on the axis of the crystal—hence, high efficiency. Note that in other focusing schemes the wavelength band and efficiency are mutually exclusive.[7] In Johann or spherically bent crystal schemes, the realization of maximum efficiency leads to a severe restriction of the recording wavelength bandwidth. However, the von Hamos scheme has high efficiency even when the spectra are recorded over a wide spectral range.

The spectra obtained with a von Hamos spectrometer form a two-dimensional image of the source for each wavelength.[6, 7] The aberrations due to off-axis source point are limited so that spatial resolution cannot, in general, exceed the source size.[7] If a CCD linear array is used as an x-ray detector, each CCD pixel integrates the radiation over the pixel height in the direction perpendicular to the dispersion (see Fig. 1). Thus, only a one-dimensional image is observed. The width of each spectral line corresponds to the source size. But, at the same time, the integration over the pixel height leads to enhanced spectrometer efficiency.

Another distinctive feature of the von Hamos geometry is that it allows the use of mosaic crystals with high integrated reflectivity. This further increase spectrometer efficiency. In this case, mosaic focusing in the direction of dispersion takes place. This results in high sensitivity without sacrificing spectral resolution.[8, 9]

3. EXPERIMENTS

3.1 Laser-produced plasmas

Laser-produced plasmas were used as x-ray sources for a CCD calibration—sensitivity, spectral response, and quantum efficiency—measurements. After the calibration procedure the CCD was used as an energy integration x-ray detector (energy integration mode). In this case the accumulated energy was measured in each pixel during one laser shot exposure. Absolute x-ray spectral measurements were performed using a focusing crystal von Hamos spectrometer and the CCD (wavelength dispersion mode). In both modes the instruments were used for laser-produced plasma diagnostics.

Laser-produced plasmas were created using two laser facilities: The "Phoenix" *Nd* glass laser (0.53 μm/10 J/2 ns) at the Lebedev Physical Institute and the "Infinity," a high-repetition rate *Nd-YAG* laser, (0.53 μm/200 mJ/3 ns/10 Hz) at Brigham Young University. The laser beam was focused onto *Mg*, *Al*, *Ti,* or *Fe* targets (see Fig. 2). The focal spot diameter was equal to ~15 μm for the Phoenix and ~40 μm for the Infinity laser.

3.2 CCD

The commercial CCD used for x-ray detection is the Toshiba model TCD 1304AP. It is a linear array with 3724 pixels. Each pixel is 8 μm wide (6 μm active) and 200 μm high. The total effective detecting area is 200 μm by 29.8 mm (8 μm x 3724 elements). The front cover glass is removed for x-ray detection. At a temperature of 20° C with an integrating time of 100 ms, the dark current noise, 3σ, is 0.5 % of the saturation value.

To prevent visible light illumination, a double *Al*-coated mylar filter (4.4 μm of mylar, 0.2 μm of *Al*) was used.

3.3 CCD calibration

The calibration procedure consists of a detector exposure by monochromatic radiation of known intensity. The comparison of the CCD signal (counts/pixel) with incidence photon flux (phot/pixel) gives the absolute CCD sensitivity, N_0 (phot/count), in each pixel at a given photon energy (or wavelength). To calibrate the CCD two x-ray sources were used—laser-produced plasmas and an Fe^{55} isotope source.

Quasi-monochromatic radiation from laser-produces plasmas was generated using a special combination of target materials and x-ray filters. The method was earlier used for calibration of the von Hamos spectrometer [9, 10] and is illustrated in Fig. 3. Targets with middle atomic numbers Z_a = 12, 13, 22 were chosen, so *[He]*- and *[H]*-like ions were effectively excited in plasmas produced by the given laser. The x-ray line radiation of the ions lies in the spectral range of interest (see Table 1). The x-ray K-absorption filters isolated a narrow spectral band with only a few lines. In this way only the radiation of resonance lines and corresponding satellites of *[H]* - and *[He]* -like ions was selected by the filters. Systematic error was caused mainly by the contribution of continuum spectra out of the separated spectral band. The line radiation filter also transmitted continuum radiation from the long-wavelength side of the *K* edge (see Fig.3: a combination of *Mg* target and *Al* filter). This contribution was estimated using a combination of an *Al* target and an *Al* filter (see Fig.3). In this case the filter transmitted only continuum radiation from the long-wavelength side of the *K* edge.

Downloaded From: http://proceedings.spiedigitallibrary.org/ on 03/27/2014 Terms of Use: http://spiedl.org/terms

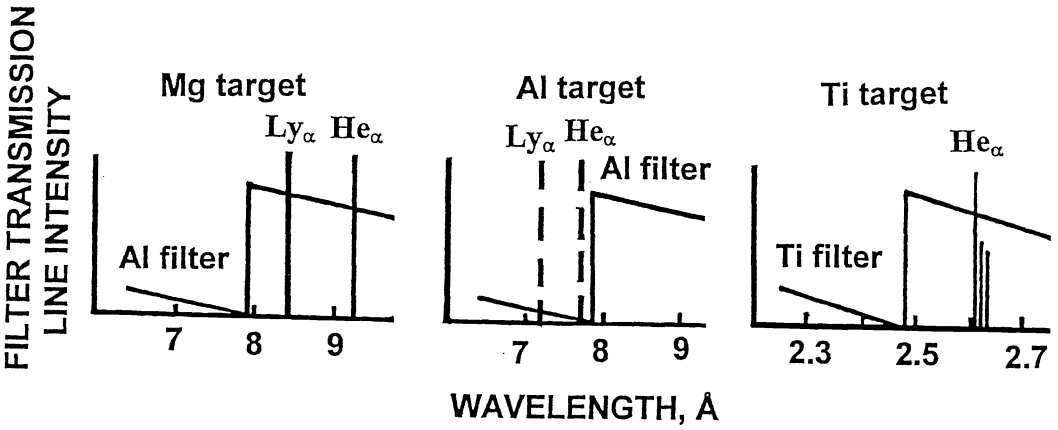


Fig .3. Principle of wavelength selection in absolute calibration experiments.

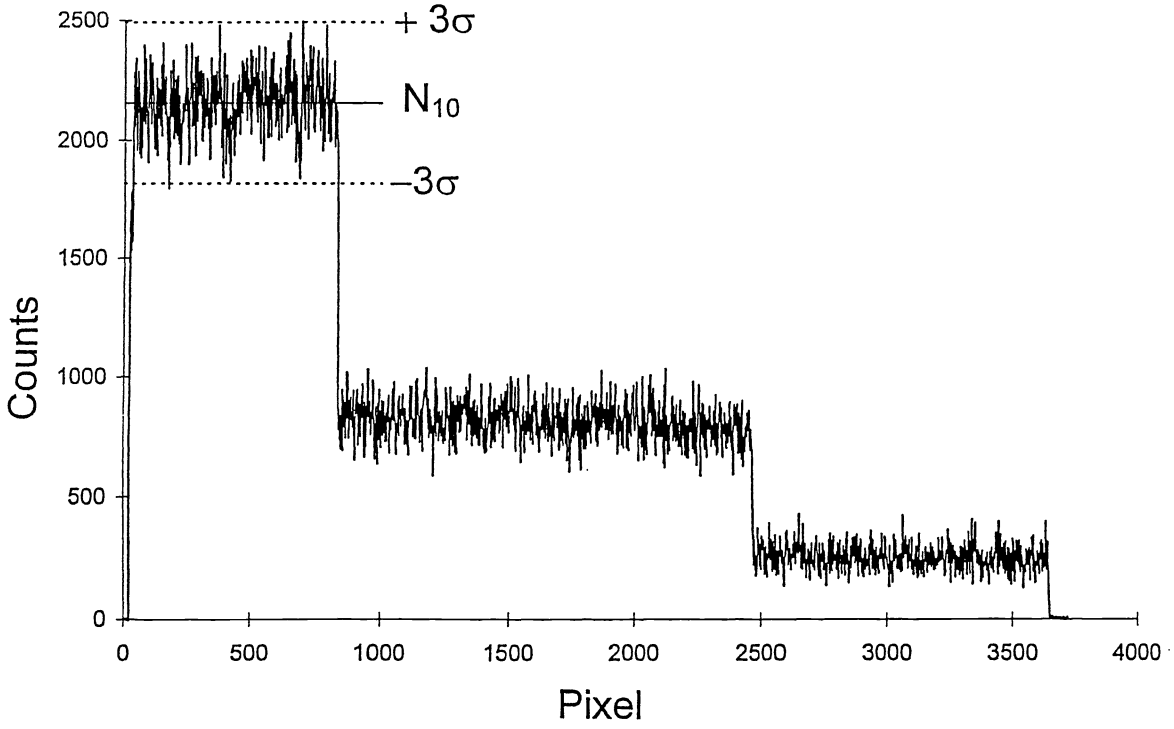


Fig. 4. Example of the CCD x-ray signal (*Mg* laser-produced plasma, CCD filters: 6.25; 12.5; 25 μm of *Al*).

Downloaded From: http://proceedings.spiedigitallibrary.org/ on 03/27/2014 Terms of Use: http://spiedl.org/terms

The measurements showed that the contribution of the continuum radiation did not exceed 20% of the line radiation intensity.

The calibration experiment scheme is shown in Fig. 2. The CCD array and a photographic film camera were installed in a vacuum chamber at the same angle with respect to the target. Both channels used the same x-ray filters which selected the needed spectral band (see Table 1). Kodak RAR 2492 x-ray photographic film measured the absolute x-ray intensity that passed through the x-ray filters using the absolute calibration data [11]. These data were compared with the CCD signal (see Fig. 4), and the absolute CCD sensitivity, N_0 (phot/count), was determined (see Table 1).

The absolute CCD sensitivity for the wavelength 2.103 Å was measured using an Fe^{55} isotope source. Preliminary to this the photon flux from the source was measured using an absolutely calibrated MOXTEK pin diode.

The noise performance of a CCD is one of the most important factors because it defines the CCD's detection limit.[2] In our case there are two major noise sources: dark current noise and photon shot noise. Our CCD driver program has the functionality of background subtraction. Fig. 5 shows the dark current signal after the background subtraction. 3σ of the noise corresponds to ~ 20 counts. This value defines the CCD's detection limit. According to the Table 1, 20 counts are equal to 3.6 phot/pixel for λ=8.4-9.2 Å, and 1.2 phot/pixel for λ=2.6 Å. These values correspond to exposures $3\cdot10^{-3}$ phot/μm^2 and $1\cdot10^{-3}$ phot/μm^2, correspondingly (pixel area is 6x200 μm^2). These exposures could be compared with the detection limit for the x-ray Kodak RAR 2492 photographic film. The film exposures for optical density D=0.1 are equal to 0.43 phot/μm^2 and 0.84 phot/μm^2 for the same wavelengths [11]. These estimations show that the CCD is 140–840 times more sensitive than the photographic film.

The other important source of noise is photon shot noise. The characteristic of this noise is that it grows when the incoming photon flux increases. The uncertainty follows a Poisson distribution and its value is proportional to the square root of number of photons, N_1, depleted in silicon.[1] The photon shot noise can be used to estimate the quantum efficiency (QE) of the CCD. In Fig. 4, the noise envelope corresponds to $\pm3\sigma$ of the measurement, where σ is the standard deviation of the measurement. Assuming the dominant noise source is photon shot noise, σ is proportional to $(N_1)^{1/2}$. The sensitivity, N_1, determined in this way is indicated in Table 1. The quantum efficiency is defined as

QE= number of photons depleted/ number of incidence photons = N_1/N_0.

The values of QE obtained are presented in the last column of Table 1. The QE values are in a good agreement with [12, 13] if we assume the Si layer thickness equals ~20 μm.

Table 1. Measured absolute values for CCD sensitivity and CCD quantum efficiency (laser-produced plasma source)

Target	Ions	Filters	Wavelength λ, Å (E, keV)	N_0, phot/count	N_1, phot/count	QE
Mg	*[H] [He]*	6.25; 12.5; 25.0 μm *Al*	8.4-9.2 Å (1.35-1.5 keV)	0.186±0.02	0.15±0.015	0.8
Ti	*[He]*	15.9; 31.8; 47.7 μm *Ti*	2.6 Å (4.8 keV)	0.065±0.007	0.056±0.006	0.9

3.4 Von Hamos spectrometer

Crystals with radius of curvature R=20 mm were used in the von Hamos spectrometer. The spectrometer axis was installed perpendicular to the laser beam (see Fig. 1). Spectra of highly charged ions were recorded using the calibrated CCD positioned in the image plane. To prevent visible light illumination, a double *Al*-coated mylar filter (4.4 μm of mylar, 0.2 μm of *Al*) was used. Spectra were recorded in a singe laser shot. To attenuate x-ray exposure on the CCD, *Al* filters of different thickness (up to 73 μm) were used. Total attenuation was up to 125 times.

Downloaded From: http://proceedings.spiedigitallibrary.org/ on 03/27/2014 Terms of Use: http://spiedl.org/terms

Initially, a mica crystal (2d=19.84 Å) was installed in the spectrometer. The spectrometer was aligned using a *He-Ne* laser, and x-ray spectra were recorded. Then a graphite crystal was installed in the same place. The crystal was made from shaped, highly oriented pyrolytic graphite (HOPG, 2d=6.708 Å) [14] and was mounted on a special cylindrical holder with the same radius of curvature (R=20 mm). Spectra were recorded for the 1st, 2nd and 5th orders of mica reflection and for the 1st order of graphite reflection. The crystal integrated reflectivity was measured in [7, 9] using laser-produced plasmas, an Fe^{55} isotope source, and a MOXTEK pin diode detector. These data, together with the CCD absolute calibration data, allowed us to record the spectra on an absolute intensity scale.

4. RESULTS

The CCD linear array itself is a very effective and useful instrument for absolute x-ray measurements and x-ray monitoring of laser-produced plasma parameters. Examples are shown in Figs. 6,7 using laser plasmas produced by the "Infinity" laser.

Fig. 6 shows the absolute x-ray intensity versus the relative position of the Mg target. Thus the focal spot diameter can be estimated. The Rayleigh range for both curves is approximately 280 μm. That corresponds to a focal spot diameter of ~40 μm. The corresponding laser intensity on the target is $I \sim 5 \cdot 10^{12}$ W/cm^2. The electron temperature T_e of the laser-produced plasma can be roughly estimated by the formula [15]

$T_e(eV)=(130)\, I^{4/9}=265$ eV,

where I is in units of 10^{12} W/cm^2. This value coincides with the T_e measurements in the Mg laser-produced plasma using the von Hamos spectrometer.

The electron temperature of laser-produced plasmas can be measured using free-free and free-bound continuum radiation transmitted through absorber foils of different elements and different thickness (absorber foil method [16]). Assuming CCD quantum efficiency is constant in the spectral range of interest, the method was applied to laser plasma produced on a polyethylene (CH_2) target. Fig. 7 gives the electron temperature T_e versus the relative position of the target. At optimal focusing, $T_e = 240 \pm 20$ eV. This value is in good agreement with the measurements mentioned above.

The x-ray spectra of highly charged ions excited in laser-produced plasmas are shown in Figs. 8-12. The plasmas were produced by the "Phoenix" laser facility. The spectra were recorded using the von Hamos spectrometer with mica (Figs. 8, 9, 11, 12) and graphite (Fig. 10) crystals.
The peak reflectivity ratio (~4) for graphite and mica crystals is in good agreement with the data [9]. The integrated reflectivity ratio for the same crystals is somewhat lower (30 versus 60 in [9]). The reason is that the CCD pixel height (200 μm) is not enough to cover the spectrum height (~350-400 μm).

X-ray spectra obtained with the mica crystal show high spectral resolution: spectral resolving power $\lambda/\delta\lambda$ was equal to 800, 2000 and 2000 for *Mg* (I[st] reflection order), *Ti* (III[rd] reflection order) and *Fe* (V[th] reflection order) for laser-produced plasmas (see Figs. 8, 9, 11, 12). The spectrum of *Ti* laser-produced plasma recorded by graphite crystal showed lower spectral resolving power: $\lambda/\delta\lambda$=200-300. This value is lower than the one demonstrated in [9] ($\lambda/\delta\lambda$=500-700) but higher than $\lambda/\delta\lambda$=50 defined by the mosaic spread of the graphite crystal. Thus, mosaic focusing takes place, but it is spread. This is caused by mosaic defocusing in the direction perpendicular to the dispersion,[9] which leads to a curved shape of the spectral lines. CCD pixels integrate the line intensity only over the pixel height.

The high spectral resolution of the mica crystal von Hamos spectrometer allowed us to observe the complete satellite structure in spectra: *w, y* – resonance and intercombination lines of the *[He]*-like ions, *k, j* – dielectronic satellites, and other (*m, s, t; q; a, r*) satellite lines (Gabriel's notation [17] for satellite lines used). The line intensity ratios were used for plasma diagnostics. Using the intensity ratio, *w/y* , the electron density, N_e, was determined for the *Mg* laser-produced plasma [18]: $N_e = 3 \cdot 10^{20}$ cm^{-3} (see Fig. 8). Using the intensity ratio of dielectronic satellites *j, k* to resonance line *w* the electron temperature T_e was measured [19] (see Figs. 8-12). The highest T_e value T_e =1400 eV was observed in the *Fe* laser-produced plasma (Fig. 12); the lowest T_e =150 eV was measured in the *Mg* laser-produced plasma. Note that the spectra were observed at very low laser pulse energies (as low as 40 mJ for *Mg* plasmas). In most cases of spectra recording it was necessary to apply a severe attenuation of the incidence intensity to avoid CCD saturation. For this reason the spectrometer is very good for studying x-ray spectra of low intensity sources: femtosecond laser-produced plasmas, micropinches, EBIT sources, etc. The spectrometer could be also used for diagnostics of laser-produced plasmas intended for EUV lithography. [20, 21]

Downloaded From: http://proceedings.spiedigitallibrary.org/ on 03/27/2014 Terms of Use: http://spiedl.org/terms

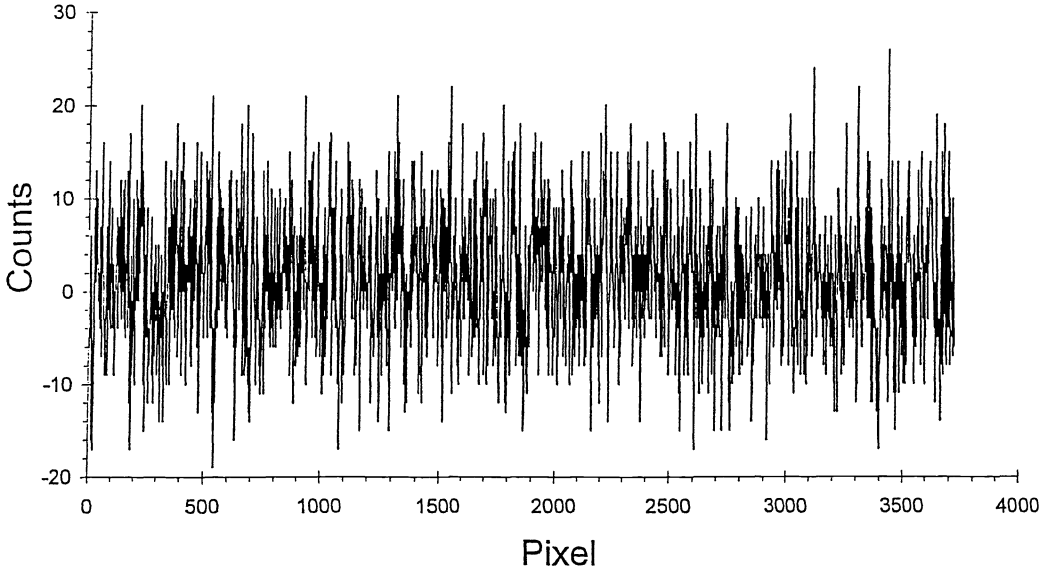


Fig. 5. Dark current distribution (noise) after background subtraction (exposure time 100 ms, CCD temperature 20° C).

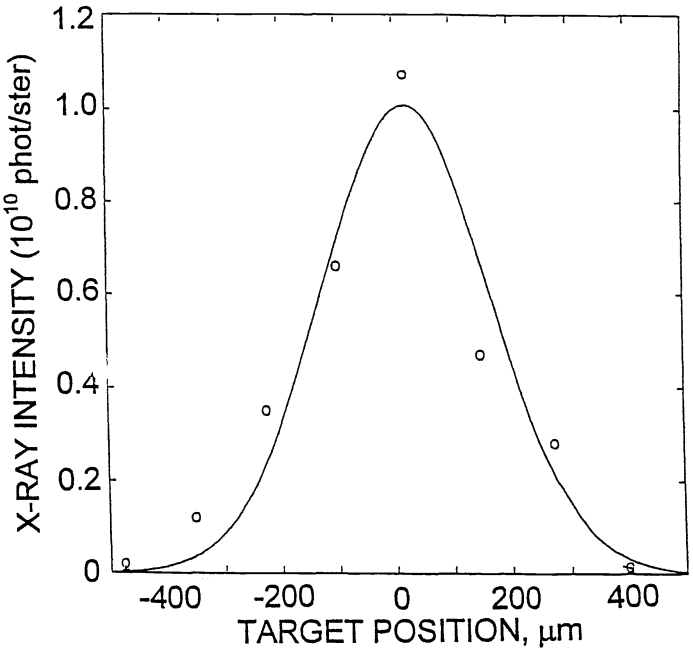


Fig. 6. Absolute x-ray yield at λ=9.2 Å from *Mg* laser-produced plasma versus relative target position (CCD filters: 12.5 μm μm of *Al*).

Downloaded From: http://proceedings.spiedigitallibrary.org/ on 03/27/2014 Terms of Use: http://spiedl.org/terms

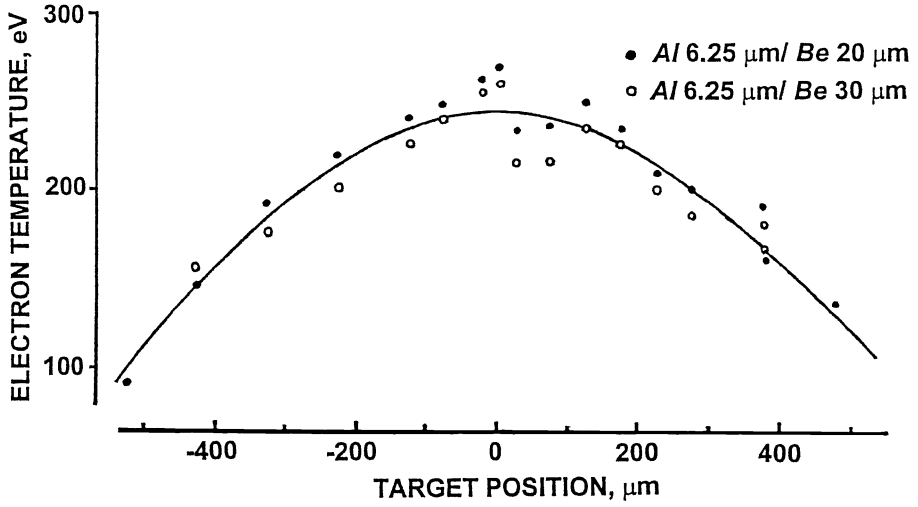


Fig. 7. Electron temperature, measured using absorber foil method, versus relative target position (CH_2 target. CCD filters: *Al/ Be*).

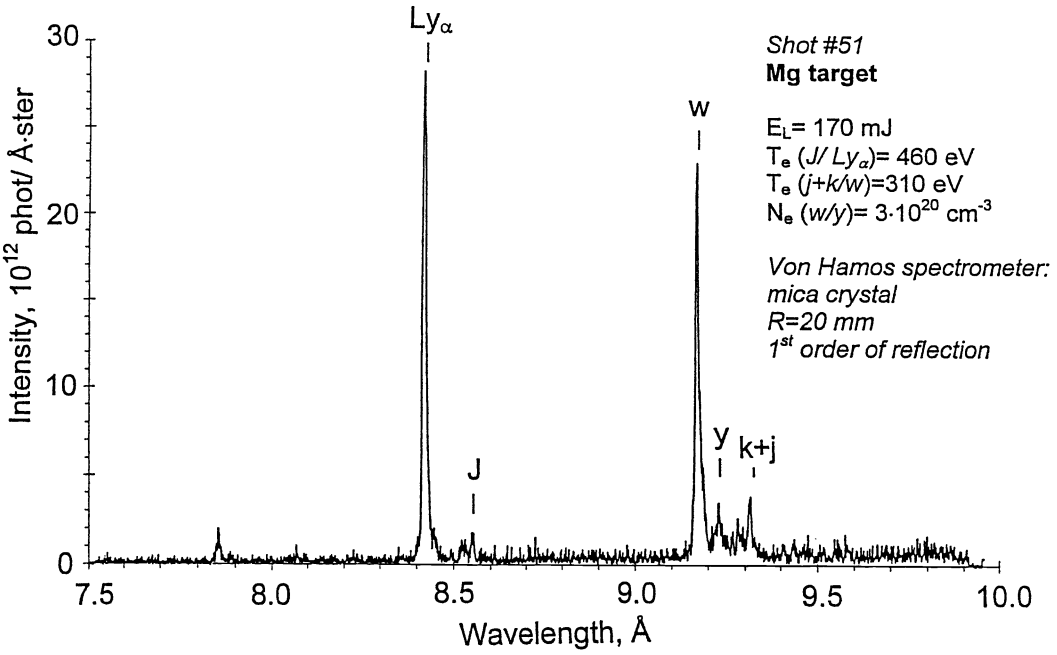


Fig. 8. Spectrum of a *Mg* laser-produced plasma.

Downloaded From: http://proceedings.spiedigitallibrary.org/ on 03/27/2014 Terms of Use: http://spiedl.org/terms

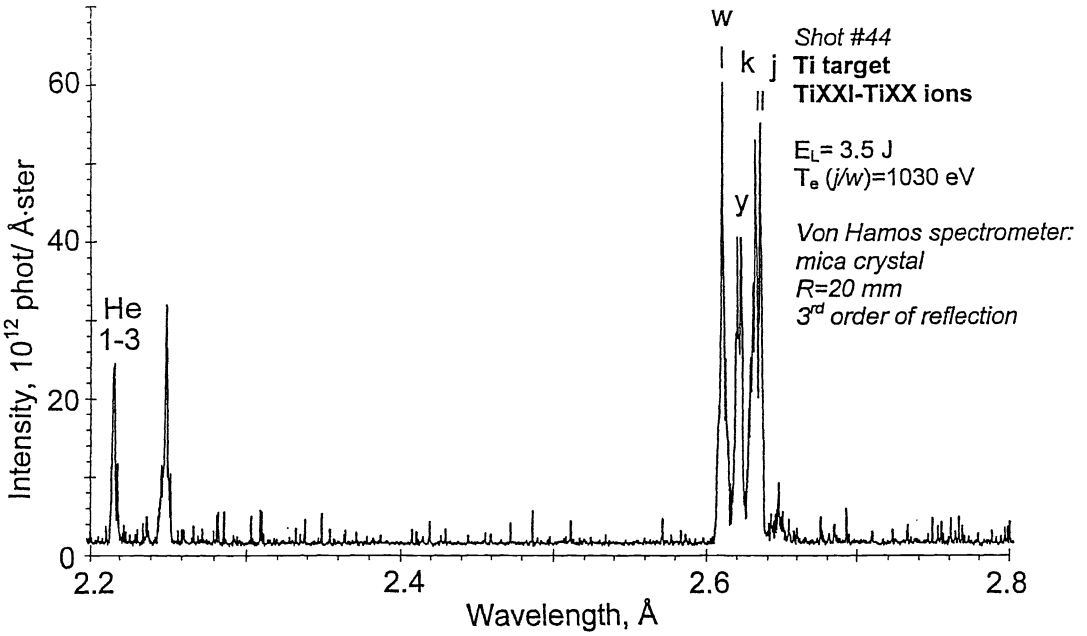


Fig. 9. Spectrum of a *Ti* laser-produced plasma.

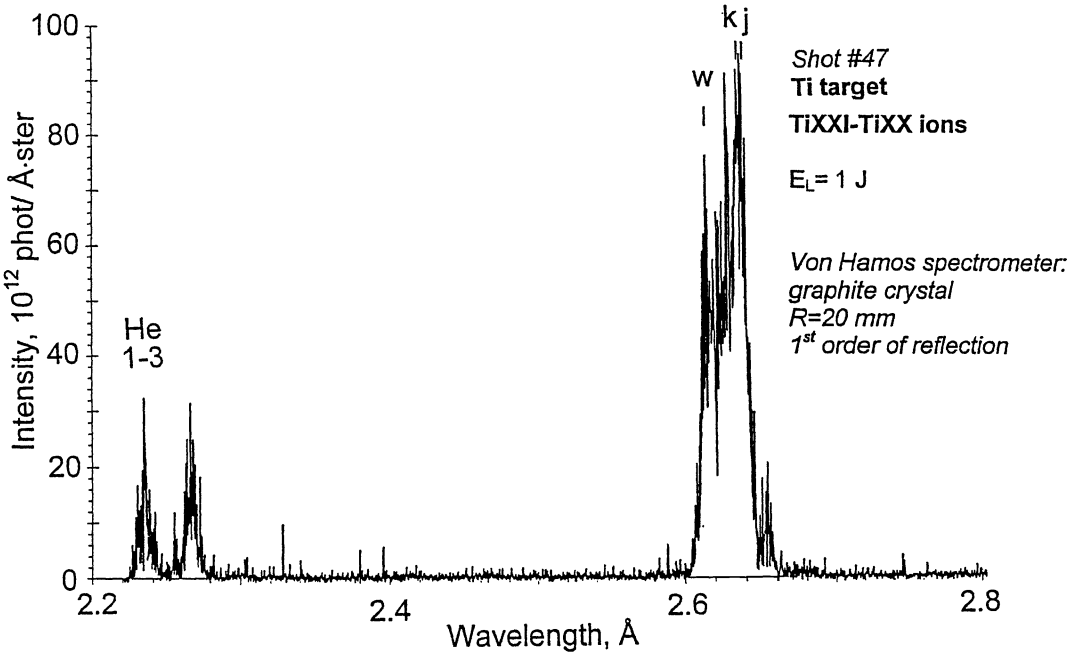


Fig. 10. Spectrum of a *Ti* laser-produced plasma.

Downloaded From: http://proceedings.spiedigitallibrary.org/ on 03/27/2014 Terms of Use: http://spiedl.org/terms

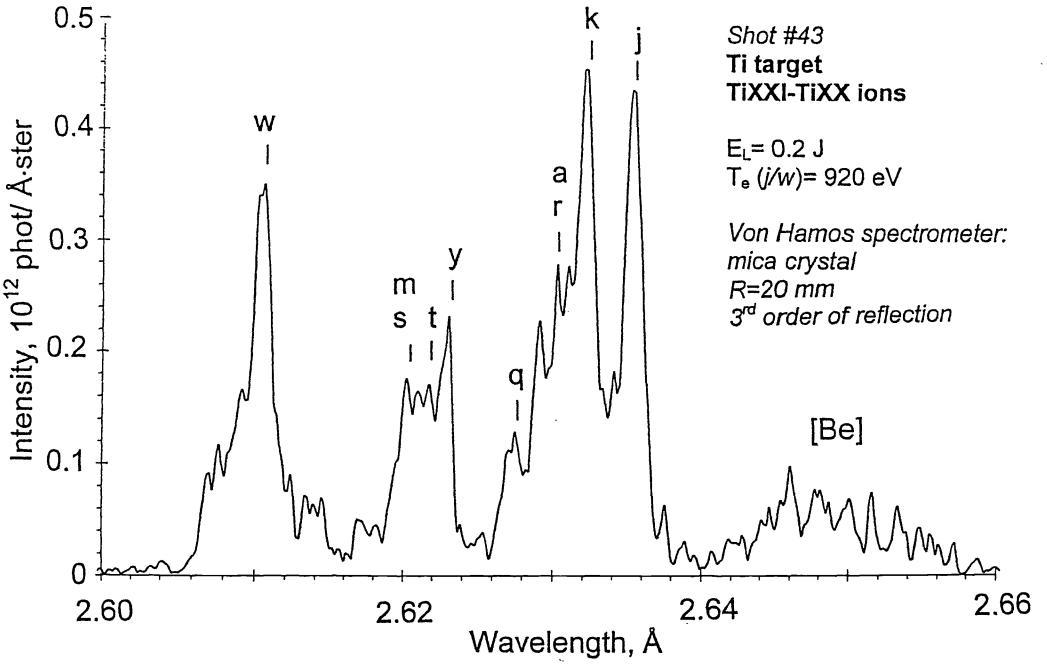


Fig. 11. Spectrum of a *Ti* laser-produced plasma in the vicinity of resonance line *w* of *[He]*-like ion.

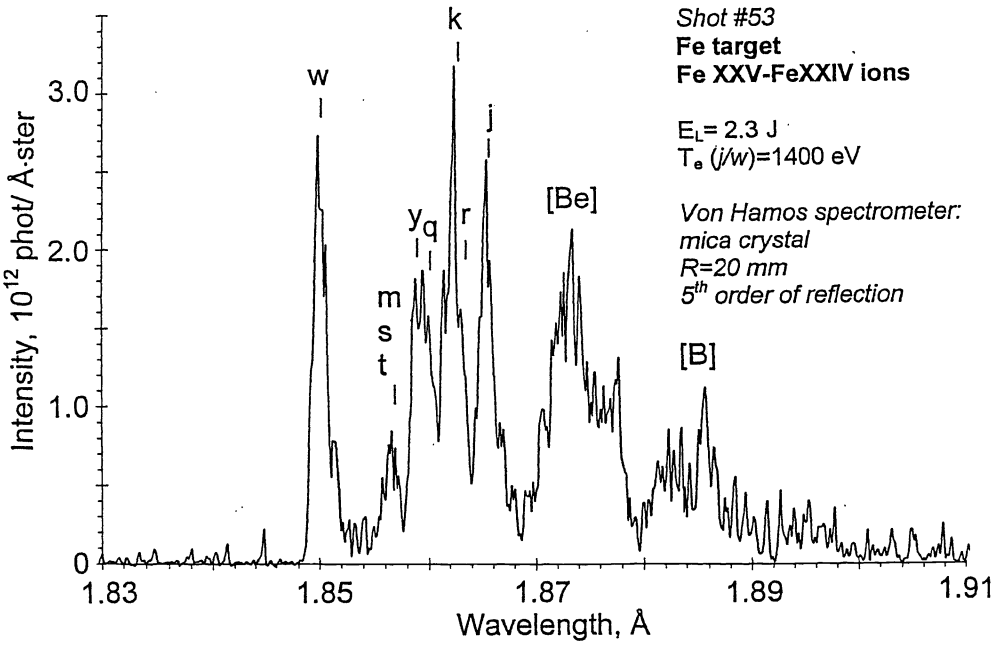


Fig. 12. Spectrum of a *Ti* laser-produced plasma in the vicinity of resonance line *w* of *[He]*-like ion.

Downloaded From: http://proceedings.spiedigitallibrary.org/ on 03/27/2014 Terms of Use: http://spiedl.org/terms

The very high efficiency of the von Hamos spectrometer with the CCD linear array as a detector makes it possible to use the device in x-ray fluorescence applications. In this case it is necessary to cool the CCD to reduce the dark current noise to measure the low photon signal during long time exposures.

ACKNOWLEDGEMENTS

The authors are grateful to E. G. Silkis (Institute of Spectroscopy) and A. A. Antonov and I. G. Grigorieva (Optigraph Company) for excellent technical help. The authors also gratefully acknowledge the invaluable assistance of Yu. S. Kasyanov and A. A. Malyutin (Institute of General Physics). This work was supported by the Brigham Young University, the P. N. Lebedev Physical Institute, and the Russian Fund for Fundamental Research (Grant No. 00-02-16632).

REFERENCES

1. *Charge-transfer devices in spectroscopy*, ed. J. V. Sweedler, K. L. Ratzlaff, and M. B. Denton, John Willey and Sons, New York, 1994.
2. A. J. D. Theuwissen, *Solid-state imaging with charge-coupled devices*, Kluwer Academic Publishers, Boston, 1995.
3. J. Dunn, B. K. F. Young, and J.Shiromizu, "X-ray sensitive charge-coupled device instrumentation for short and ultrashort pulse laser-produced plasma experiments," *Rev. Sci. Instrum.* **66**, pp. 706-708, 1995.
4. M. Koenig, J. M. Boudenne, P. Legriel, A. Benuzzi, T. Grandpierre, D. Batani, S. Bossi, S. Nicolella, and R. Benattar "A computer driven crystal spectrometer with charge coupled device detectors for x-ray spectroscopy of laser plasmas," *Rev. Sci. Instrum.* **68**, pp. 2387-2392, 1997.
5. F. Blasco, C. Stenz, F. Salin, A. Ya. Faenov, A. I. Magunov, T. A. Pikuz, and I. Yu. Skobelev, "Portable, tunable, high-luminosity spherical crystal spectrometer with an x-ray charge coupled device, for high-resolution x-ray spectromicroscopy of clusters heated by femtosecond laser pulses," *Rev. Sci. Instrum.* **72**, pp. 1956-1962, 2001.
6. Von L. v. Hámos, "Röntgenspektroskopie und Abbildung mittels gekrùmmter Kristallreflektoren," *Ann. Phys.* **17**, pp. 716-724, 1933.
7. A. P. Shevelko, "X-ray spectroscopy of laser-produced plasmas using a von Hamos spectrograph," *SPIE* **3406**, pp. 91-108, 1998.
8. B. Yaakoby and A. J. Burek, "Crystal Diffraction Systems for X-Ray Spectroscopy, Imaging, and Interferometry of Laser Fusion Targets," *IEEE QE* **19**, pp. 1841-1854, 1983.
9. A. P. Shevelko, A. A. Antonov, I. G. Grigorieva, Yu. S. Kasyanov, L. V. Knight, A. Reyes-Mena, C. Turner, Q. Wang, and O. F. Yakushev, "A Focusing Crystal von Hamos Spectrometer for X-ray Spectroscopy and X-ray Fluorescence Applications," *SPIE* **4144**, pp. 148-154, 2000.
10. F. Bijkerk, E. Louis, G. E. van Dorssen, A. P. Shevelko, and A. A. Vasilyev, "Absolute brightness of laser plasmas in the soft-x-ray emission band," *Appl. Opt.* **32**, pp. 4247-4252, 1993.
11. B. L. Henke, F. G. Fujiwara, M. A. Tester, C. H. Dittmore, and M. A. Palmer, "Low-energy x-ray response of photographic films. II. Experimental characterization," *J. Opt. Soc. Am.* **B1**, pp. 828-849, 1984.
12. A. Saemann and K. Eidmann, "Absolute calibration of a flat field spectrometer in the wavelength range 10-70 Å," *Rev. Sci. Instrum.* **69**, pp. 1949-1954, 1998.
13. L. Poletto, A. Boscolo, and G. Tondello, "Characterization of a charge-coupled-device detector in the 1100-0.14-nm (1-eV to 9-keV) spectral region," *Appl. Opt.* **38**, pp. 29-36, 1999.
14. A. A. Antonov, V. B. Baryshev, I. G. Grigoryeva, G. N. Kulipanov, and N. N. Shchipkov, "Focusing shaped pyrographite monochromators in synchrotron radiation experiments," *Nucl. Instrum. and Meth.* **A308**, pp. 442-446, 1991.
15. C. Yamanaka, T. Yamanaka, T.Sasaki, J. Mizui, and H. B. Kang, "Brillouin Backscattering and Parametric Double Resonance in Laser-Produced Plasma, " *Phys. Rev. Lett.* **32**, pp. 1038-1041, 1974.
16. F. C. Jahoda, E. M. Little, W. E. Quinn, G. A. Sawyer, and T. F. Stratton, "Continuum Radiation in the X Ray and Visible Regions from a Magnetically Compressed Plasma (Scylla)," *Phys. Rev.* **119**, pp. 843-856, 1960.
17. A. H. Gabriel, "Dielectronic satellite spectra for highly charged helium-like ion lines," *Mon. Not. R. Astron. Soc.* **160**, pp. 99-119, 1972.
18. A. V. Vinogradov, I. Yu. Skobelev, and E. A. Yukov, "Determination of plasma density from spectra of heliumlike ions," *Sov. J. Quant. Electron.* **5**, pp. 630-633, 1975.
19. L. A. Vainshtein, U. I. Safronova, and A. M. Urnov, "Dielectronic satellites of resonance lines of highly charged ions," *Proceedings of the Lebedev Physical Institute, Nova Science publishers*, ed. N. G. Basov, **119**, 1980.

Downloaded From: http://proceedings.spiedigitallibrary.org/ on 03/27/2014 Terms of Use: http://spiedl.org/terms

20. G. Kubiak, L. J. Bernardez, K. Krenz, W. C. Replogle, W. C. Sweatt, D. W. Sweeney, R. M. Hudyma, and H. Shields, "High-power source and illumination system for extreme ultraviolet lithography," *SPIE* **3767**, pp. 136-142, 1999.
21. R. C. Constantinescu, J. Jonkers, P. Hegeman, and M. Visser, "A laser-generated water plasma source for extreme-ultraviolet lithography and at-wavelength interferometry," *SPIE* **4146**, pp. 101-112, 2000.

Downloaded From: http://proceedings.spiedigitallibrary.org/ on 03/27/2014 Terms of Use: http://spiedl.org/terms